Applied and Environmental Microbiology, Sept. 2006, p. 5702–5712 Vol. 72, No. 9
0099-2240/06/$08.00+0 doi:10.1128/AEM.02982-05

Biological Filtration Limits Carbon Availability and Affects Downstream Biofilm Formation and Community Structure†

Chee Meng Pang[1] and Wen-Tso Liu[2]*

Department of Civil Engineering, National University of Singapore,[1] and Division of Environmental Science and Engineering, National University of Singapore,[2] Singapore

Received 17 December 2005/Accepted 24 May 2006

Carbon removal strategies have gained popularity in the mitigation of biofouling in water reuse processes, but current biofilm-monitoring practices based on organic-carbon concentrations may not provide an accurate representation of the in situ biofilm problem. This study evaluated a submerged microtiter plate assay for direct and rapid monitoring of biofilm formation by subjecting the plates to a continuous flow of either secondary effluent (SE) or biofilter-treated secondary effluent (BF). This method was very robust, based on a high correlation ($R^2 = 0.92$) between the biomass (given by the A_{600} in the microtiter plate assay) and the biovolume (determined from independent biofilms developed on glass slides under identical conditions) measurements, and revealed that the biomasses in BF biofilms were consistently lower than those in SE biofilms. The influence of the organic-carbon content on the biofilm community composition and succession was further evaluated using molecular tools. Terminal restriction fragment length polymorphism analysis of 16S rRNA genes revealed a group of pioneer colonizers, possibly represented by *Sphingomonadaceae* and *Caulobacter* organisms, to be common in both SE and BF biofilms. However, differences in organic-carbon availabilities in the two water samples eventually led to the selection of distinct biofilm communities. Alphaproteobacterial populations were confirmed by fluorescence in situ hybridization to be enriched in SE biofilms, while *Betaproteobacteria* were dominant in BF biofilms. Cloning analyses further demonstrated that microorganisms adapted for survival under low-substrate conditions (e.g., *Aquabacterium*, *Caulobacter*, and *Legionella*) were preferentially selected in the BF biofilm, suggesting that carbon limitation strategies may not achieve adequate biofouling control in the long run.

The aggregation of microbial life into sessile biofilm communities is ubiquitous in aquatic environments. In the water treatment industry, biofilms are reviled for their adverse effects on water quality, pipeline corrosion, and disinfectant consumption (8). For water reuse systems, biofilms can also cause significant reduction in water production for membrane-based water purification processes (40). As biofilms in these systems accumulate at inaccessible locations, monitoring often depends on surrogate parameters, like organic-carbon content. However, the relationship between organic-carbon concentrations and bacterial growth in biofilms is not always straightforward. For example, although disinfected water with an assimilable-organic-carbon (AOC) concentration of less than 50 μg C/liter is commonly accepted as biologically stable (26), the formation of biofilms has still been observed on pipe surfaces exposed to potable waters with AOCs as low as 39 μg C/liter (33). Despite this uncertainty, biofilm monitoring has continued to rely largely on organic-carbon-based measurements, since simple and convenient-to-use alternatives for direct biofilm quantification are unavailable.

While the relationship between the organic-carbon concentration and downstream biofilm formation has often been assumed to be highly correlated in the water reuse industry, the effects of the carbon content on the resultant biofilm architecture and community composition have been largely overlooked. Such insight can be important, however, because it allows early intervention (such as in the case of pathogen detection) and assists in the assessment of existing control strategies. Microscopy flow cell studies assessing the influence of the organic-carbon concentration on biofilm structure have indicated that the biofilm architecture is structurally adaptive to changes in carbon concentrations (41). Unfortunately, the conditions used are not ecologically relevant to water reuse systems in terms of the model organisms examined, the concentration levels, and the substrate type. Indeed, biofilm architecture and community structure are believed to be determined functionally (11) by conditions such as the nature of the available carbon source (19).

This communication considers the effect of the organic-carbon content in a context relevant to water reuse environments. Direct biofilm quantification is achieved using a novel system of submerged microtiter plates. To evaluate the applicability of this method, secondary effluent (SE) from a local activated-sludge plant was treated using biological filtration (BF), and microtiter plates were exposed under continuous flow to allow biofilm formation in the two effluents. The reliability of this method was assessed by comparing the biomasses in these plates to those of independent biofilm samples developed on glass slides. At the same time, molecular biology tools addressing temporal changes in the architectures and community com-

* Corresponding author. Mailing address: Division of Environmental Science and Engineering, National University of Singapore, Block E2, No. 04-07, 1 Engineering Drive 2, Singapore 117576. Phone: (65) 65161315. Fax: (65) 67744202. E-mail: eseliuwt@nus.edu.sg.

† Supplemental material for this article may be found at http://aem.asm.org/.

positions of SE and BF biofilms were investigated in relation to organic-carbon limitation imposed by biofiltration.

MATERIALS AND METHODS

Biofilter setup and operation. Secondary effluent was obtained from a local wastewater treatment plant. As the effluent served as the feed to a biofilter, it was continuously aerated to maintain a dissolved-oxygen level of about 6.0 mg/liter. Periodic monitoring of pHs ranging from 6.8 to 7.5 indicated that pH adjustments were not necessary. The biofilter consisted of a column packed with washed coarse sand (effective size, 2.4 mm; uniformity coefficient, 1.2) and was in operation for two consecutive experimental periods, designated run 1 (84 days) and run 2 (98 days). During each run, the biofilter was operated at an empty-bed contact time of 20 min and a discharge rate of 20 ml/min at room temperature (28 to 30°C). Backwash was carried out once every 2 days for 10 min to prevent excessive head loss.

Effluent from the biofilter was used to irrigate a flow channel containing sterile microtiter plates and glass slides. Another flow channel was irrigated with the secondary effluent without further treatment. The average effluent velocity in these flow channels was 0.27 cm/min, and stagnation conditions did not occur within the wells of microtiter plates when a dye was used to trace the hydraulic-flow profile in the flow channel. Microtiter plates and glass slides (for fluorescence in situ hybridization [FISH] and DNA extraction) were sampled on alternate days over a 12-day period beginning on days 72 and 86 for runs 1 and 2, respectively. BF_2 and SE_6 denote biofilms cultivated on biofilter effluent on day 2 and secondary effluent on day 6, respectively.

Chemical analyses. The secondary effluent and biofilter effluent were filtered through a 0.45-μm polycarbonate filter before chemical analyses. The dissolved organic carbon (DOC) content was determined regularly in triplicate over the entire duration of runs 1 and 2 using a Model 101 Wet Oxidation Total Carbon Analyzer (O. I. Analytical, College Station, Texas) in accordance with standard methods (2). Ammonia, nitrate, nitrite, phosphate, and sulfate were analyzed only in run 2 whenever biofilm samples were collected. Their concentrations were measured by ion chromatography using a DX500 chromatography system (Dionex, Sunnyvale, Calif.) as described previously (2).

Microtiter plate assay. Duplicate microtiter plates (Nunc, Roskilde, Denmark) in each flow channel were collected, and the biofilm biomasses on the walls and the bottom of individual wells were determined as described previously (12, 35). In brief, 25 μl of 1% crystal violet dye was added to stain the biofilm cells. After an incubation of 45 min, the contents of each well were gently aspirated and discarded. The wells were then washed three times with sterile ultrapure water to remove the excess dye. The dye that stained the biofilm biomass was subsequently solubilized in 95% ethanol for another 45 min; 125 μl of this dye was transferred to a new microtiter plate, and its absorbance at 600 nm (A_{600}) was determined using a Sunrise Remote Control Microtiter Plate Reader and Magellan software (version 3.0).

Fluorescence in situ hybridization. Biofilms on glass slides were fixed in 4% paraformaldehyde or 50% ethanol. To preserve their structural integrity, the biofilms were embedded with a thin layer of polyacrylamide gel (10). The cyanine 3 (Cy3)-labeled oligonucleotide probes EUB338I/II/III, ALF1b, BET42a, GAM42a, CF319a, and HGC69a were hybridized individually to the embedded biofilms at 46°C for 3 h under the stringency conditions appropriate for each probe (45). Hybridization with Cy3-labeled BET42a (or GAM42a) probe was coupled with hybridization with an unlabeled GAM42a (or BET42a) competitor to insure specificity. The samples were then stained with the fluorescent DNA dye SYTO 9, part of the Live/Dead BacLight Bacterial Viability Kit (Molecular Probes, Eugene, Ore.), according to the manufacturer's instructions.

Microscopy and image analysis. Microscopic images of hybridized/stained biofilms were acquired using a confocal laser scanning microscope (CLSM) model LSM 5 Pa (Carl Zeiss, Jena, Germany) (45) under a Plan-Apochromat 63×/1.4-numerical-aperture oil immersion objective lens. Images of STYO 9-stained cells were acquired at an excitation of 488 nm and emission of 505 to 530 nm, while signals from Cy3-conjugated probes were acquired at an excitation of 543 nm with a long-pass emission filter at 560 nm. At least eight microscopic fields (corresponding to a total area of $>1.7 \times 10^5$ μm^2) was acquired to obtain statistically valid determinations of cell numbers within intact biofilms (20). Quantitative biofilm parameters were computed with COMSTAT (16), and as described previously, the biovolume was defined as the number of positive pixels in a CLSM image stack multiplied by the voxel size ($\sim 70 \times 10^{-3}$ μm^3 in this case) and divided by the area covered in the field of view (2.2×10^4 μm^2).

Total-community DNA extraction. Glass slides containing the biofilm sample were removed from the flow channel and immediately transferred into sterile 1× phosphate-buffered saline (PBS) solution. To remove loosely adhering cells, the glass slides were rinsed three times in 1× PBS. The biofilm cells were then resuspended in 1× PBS using a probe sonicator (Vibracell; Sonics) operated at 4 W over five 10-s bursts. Residual biofilm material on the glass slide was physically removed using sterile cotton buds and resuspended by vortexing it. The biofilm materials obtained from sonication and the sterile cotton buds were pooled and collected by centrifugation at 16,440 × *g* for 10 min. The cell pellets were then stored at −80°C. Total-community DNAs were subsequently extracted as described elsewhere (30).

T-RFLP. Total-community DNAs of the biofilm samples were amplified by PCR using the *Bacteria*-specific forward primer 47F (5′ Cy5-CYT AAC ACA TGC AAG TCG-3′) and the reverse primer 927R (5′-ACC GCT TGT GCG GGC CC-3′) (9). To remove single-stranded DNA that could contribute to the generation of pseudo-terminal restriction fragments, PCR-amplified products were digested with mung bean nuclease (New England BioLabs, Beverly, Mass.) (13). The resulting PCR products were purified using a QIAquick PCR purification kit (QIAGEN, Chatsworth, Calif.) and digested separately using three different tetrameric restriction enzymes, MspI, RsaI, and HhaI (New England BioLabs, Beverly, Mass.), at 37°C for 3 h. Terminal restriction fragment length polymorphism (T-RFLP) was performed according to a previously described protocol (30) in a model CEQ 8000 automated sequencer (Beckman Coulter, Fullerton, Calif.). T-RFLP fingerprints for each sample were obtained based on the average fingerprinting profiles of two separate analyses. Clustering of different T-RFLP fingerprints and other statistical analyses were performed using MINITAB Statistical Software, release 14. The Hellinger distance was calculated from the Euclidean distance after square root transformation of relative peak areas (27). A distance matrix based on the Hellinger distance was computed, and a dendrogram was generated using Ward's hierarchical-clustering method.

16S rRNA gene clone libraries and phylogeny analysis. 16S rRNA gene clone libraries were constructed only for biofilm samples SE_10 and BF_10. Total-community DNA was amplified using a bacterial primer set, EUB008F (5′-AGA GTT TGA TCC TGG CTC AG-3′) and 1512R (5′-GGC TAC CTT GTT ACG ACTT-3′), in an iCycler thermal cycler (Bio-Rad, Hercules, Calif.) (9). PCR cycling conditions and the construction of clone libraries were as described previously (29). The partial sequences (>1,300 bp) obtained from representative clones were then compared to 16S rRNA gene sequences in GenBank using the NCBI BLAST program (1). Chimeric artifacts were detected using the CHECK-CHIMERA tool available at the Ribosomal Database Project (31), as well as the Pintail program (3). The phylogenetic tree was prepared in MEGA3 (21) by applying the neighbor-joining algorithm (1,000 bootstrap replicates) to the Jukes-Cantor distances computed for the aligned sequences.

Nucleotide sequence accession numbers. The sequences in this study were submitted to GenBank under accession numbers DQ327673 to DQ327700.

RESULTS

Performance of the biofilter treating secondary effluent. As the concentration of DOC in the SE effluent is generally low (<13 mg/liter), a lag period was necessary to accumulate sufficient biomass within the biofilter. Stable DOC removal of greater than 5% was achieved after 50 days in run 1 and 40 days in run 2 (Fig. 1). During subsequent operations, DOC concentrations in the biofilter effluent ranged from 5 to 10 mg/liter, while DOC removal efficiencies fluctuated between 5 and 15% in both runs.

On day 72 in run 1 and day 86 in run 2, biofilm samples were collected from microtiter plates and glass slides over a period of 12 days. In this period, commonly reported water quality parameters were also monitored (Table 1). Statistically significant depletion of DOC and dissolved oxygen was observed (both *P* values were 0.000 in a paired *t* test), suggesting that the predominant form of catabolism in the biofilter was aerobic carbon oxidation. No significant reduction in NH_4^+-N, NO_3^--N, NO_2^--N, PO_4^{3-}-P, or SO_4^{2-} occurred as a result of biofiltration (all *P* values were >0.05).

Biofilm biomass, as estimated by microtiter plate assay. The biofilm biomass developed in microtiter plates is given by an A_{600} measurement, and the results over 12 days are shown in

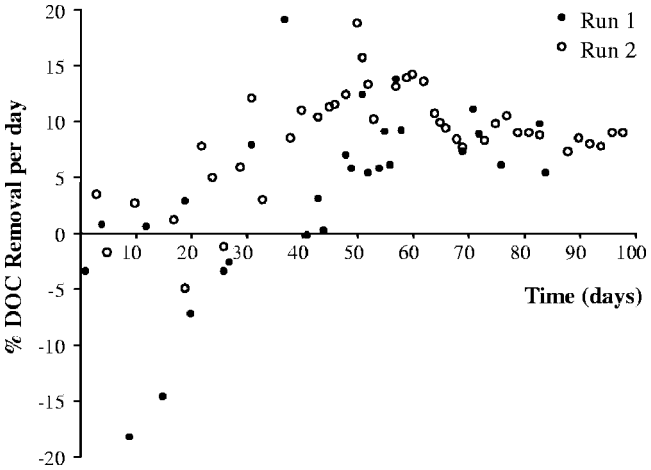

FIG. 1. DOC removal efficiencies of the biofilter over the entire duration of runs 1 and 2.

Fig. 2. In run 1, both SE and BF biofilms followed similar trends, and the A_{600} consistently increased over the 12-day period. Using Tukey's method for pairwise comparison, a significant increase (defined as an α of 0.05) in the A_{600}s for both biofilms occurred every 4 days (e.g., the A_{600} on day 12 was statistically higher than the A_{600} obtained on day 8 and earlier, but not that on day 10). However, a different pattern was observed in run 2. In the case of SE biofilms, the A_{600}s on days 8 and 12 were significantly higher than those obtained on days 2 to 6, suggesting a gradual buildup of biomass. For BF biofilms, no significant difference in the A_{600} was observed in all cases, except between days 2 and 8. To evaluate the effect of carbon limitation, the A_{600} was found to be significantly reduced when biofilms were cultivated in the BF effluent (P = 0.000 in a paired t test).

Biofilm development dynamics and quantitative biofilm analyses. Microscopic observations of developing biofilms in run 2 (Fig. 3) showed a distinct difference in biofilm morphology. When cultivated on SE, the biofilm structure underwent clearly defined changes. The biofilm first developed as a single layer of cells, although microcolonies could be observed as early as day 2 (Fig. 3). Larger aggregates containing different morphotypes were subsequently formed (day 6). These aggregates grew in size, and by day 12, the biofilm consisted of individual bacterial cells interspersed between colonies of various sizes. The overall biofilm morphology appeared patchy and heterogeneous. In contrast, the biofilm developed on BF consisted of a monolayer of cells. Although the number of single cells increased over the 12-day period, well-defined microcolonies were not observed. The overall biofilm structure remained flat, with bacterial cells randomly distributed over the glass substratum.

Image analyses performed on CLSM optical stacks provided quantitative measures of biovolume, average thickness, surface coverage, and cell surface area-to-biovolume (S/B) ratios (Fig. 4). Although the biovolume and average thickness generally increased over time in both runs, the development of BF biofilms was affected by organic-carbon removal. Compared to their SE counterparts, the BF biofilms had significantly smaller biovolumes (P = 0.005 in a paired t test) and thickness (P = 0.006). Furthermore, biovolume measurements and A_{600}s obtained in run 1 were, to some extent, higher than those encountered in run 2. Given the identical experimental conditions (e.g., temperature, empty bed contact time, backwash conditions, dissolved-oxygen levels, and flow channel velocities) used in both runs, this inconsistency might have been related to random variations in the quality of the SE. One possibility is that larger amounts of suspended solids were encountered in run 1. This could enhance biofilm formation by serving as both an inoculum source and a substrate and thus produce biofilms with increased spatial size (as reflected by the biovolume and A_{600}) in run 1.

In terms of surface coverage, both SE and BF biofilms tended to colonize a larger percentage of the substratum over time, but no significant difference in this parameter was detected between the two biofilms (P = 19.6). The S/B ratio typically declined over the experimental period, suggesting that the biofilms might have become more compact over time. A notable exception to this was the BF biofilm in run 2, for which an increase in the S/B ratio was observed. In addition, high correlations ($R^2 > 0.92$) were obtained between A_{600} and biovolume measurements (see Fig. S1 in the supplemental material), suggesting that relatively good inferences of biovolume could be drawn from the A_{600} values.

Biofilm community structure as revealed by FISH. FISH analyses of SE and BF biofilm samples showed that 70% to 80% of the cells stained by SYTO 9 could be hybridized using the *Eubacteria* probe mix. Using five different phylum and subphylum level probes, consistent trends in the community structures of SE biofilms were observed in both runs (Fig. 5). At days 2 and 4, *Betaproteobacteria* were most abundant, at >30%. *Alphaproteobacteria*, *Gammaproteobacteria*, and *Actinobacteria* were present at between 10% and 20%, while bacteria affiliated with the *Cytophaga-Flexibacter-Bacteroides* (CFB) cluster were minor members of the biofilm community (~5%). Between day 6 and day 10, the abundances of *Alphaproteobacteria* and CFB cluster members gradually increased, and this was accompanied by a concurrent decrease in the numbers of *Betaproteobacteria* and *Actinobacteria*. By day 12, *Alphaproteobacteria*, accounting for about 30% of the biofilm biomass, replaced *Betaproteobacteria* (~20%) as dominant members of the SE biofilm community. *Gammaproteobacteria* remained in the range of 10% to 20% over the 12-day period.

TABLE 1. Performance of biofilter over the 12-day experimental period in run 2[a]

Parameter (mg/liter where applicable)	SE (biofilter influent)	BF
DOC	8.7 ± 0.3	8.0 ± 0.3
% DOC removal per day	NA[b]	8.2 ± 0.7
Dissolved oxygen	6.3 ± 0.2	4.1 ± 0.4
NH_4^+-N	6.0 ± 0.4	5.6 ± 0.4
NO_3^--N	5.6 ± 0.3	6.5 ± 0.2
NO_2^--N	0.9 ± 0.4	0.5 ± 0.0
PO_4^{3-}-P	3.2 ± 0.0	3.0 ± 0.1
SO_4^{2-}	66.5 ± 0.6	69.6 ± 2.7
pH	7.3 ± 0.2	6.9 ± 0.1

[a] The average value for six water samples is shown, together with the standard deviation.
[b] NA, not applicable.

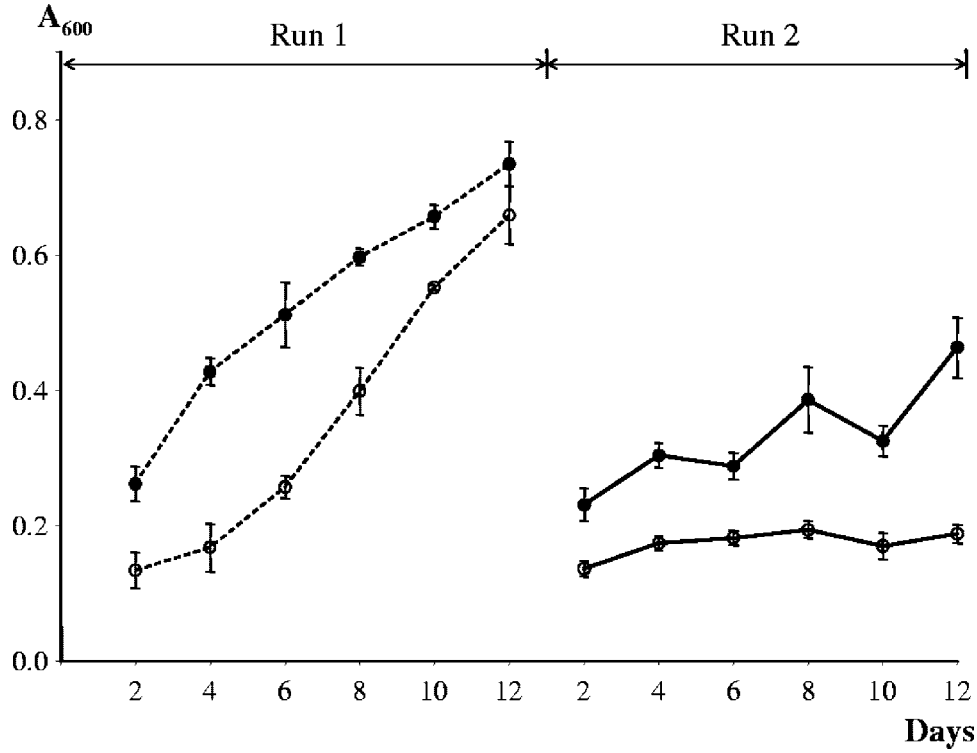

FIG. 2. Average A_{600}s obtained from the microtiter plate assay for biofilms developed using secondary effluent (●) and biofilter effluent (○). The error bars indicate the standard deviations.

For BF biofilms, the community structure did not change considerably over the 12-day period, during which *Betaproteobacteria* were the most abundant (>30%). *Gammaproteobacteria* were present at between 10% and 20% of the biofilm community, while the CFB cluster generally accounted for <10%. There was an enrichment of *Alphaproteobacteria* in run 2, but this was not observed in run 1.

Biofilm community structure as revealed by 16S rRNA gene clone libraries. The 108 clones from the SE_10 biofilm were assigned to 18 phylotypes, in which *Alphaproteobacteria* were the most dominant (35%), followed by *Betaproteobacteria* (27%) and those bacteria affiliated with the CFB group (10%). Two phylotypes related to candidate division TM7 were found (9.3%), and a single phylotype each for *Gammaproteobacteria* (6.5%), *Actinobacteria* (5.6%), and *Firmicutes* (3.7%) were also present. For the BF_10 biofilm, 19 phylotypes were identified from 114 clones. *Betaproteobacteria* were the most dominant (41%), followed by *Alphaproteobacteria* (24%) and *Gammaproteobacteria* (15%). In addition, a *Spirochaetes*-related phylotype (13%) and two others affiliated with candidate division TM7 (3.5%) were also detected.

The phylogenetic relationship between *Proteobacteria* phylotypes and those from the CFB cluster was established (Fig. 6). Alphaproteobacterial phylotypes were predominantly related to the *Sphingomonadaceae* in the SE_10 biofilm, and this contrasted with the dominance of *Caulobacter*-related clones in the BF_10 biofilm. In the case of *Betaproteobacteria*, the *Acidovorax*-related phylotypes SE191 and BF192 were the most abundant. The BF_10 biofilm also contained phylotypes BF23 and BF87, which were closely related to *Aquabacterium*, a genus commonly associated with biofilms of drinking water systems (18). The nitrogen-fixing *Azospira oryzae* (39) phylotypes BF160 and BF161 were also observed in the BF_10 biofilm, but not in the SE_10 biofilm. The gammaproteobacterial phylotype SE153 was related to *Acinetobacter*, but those from the BF_10 biofilm (BF74, BF89, and BF115) were related to *Legionella* instead.

Biofilm community structure as revealed by T-RFLP. MspI-, RsaI-, and HhaI-digested T-RFLP fingerprints all showed that biofilm communities retrieved on days 2 and 4 tended to be more diverse than those retrieved after 6 days and longer. MspI-digested T-RFLP patterns (Fig. 7) showed that the fingerprints of both SE_2 and BF_2 were characterized by the occurrence of a large number (~30) of minor terminal restriction fragments (T-RFs), a few of which accounted for more than 10% of the total biofilm community. Most of these T-RFs declined in abundance after day 6. A notable exception was the 111-bp T-RF, which became the dominant T-RF in both samples. At the end of 12 days, the number of detectable T-RFs decreased to <15, reflecting a loss in species richness in both biofilm communities.

Differences in the distributions of T-RFs were also observed between SE and BF fingerprints. For example, the BF_6 and BF_10 biofilms contained T-RFs of 100 and 130 bp, both of which were absent in the SE_6 and SE_10 biofilms. The 500-bp T-RF was consistently detected in the SE biofilms but was not found in any BF samples. To better describe patterns of variation between T-RFLP profiles, fingerprints generated from the restriction enzymes MspI, RsaI, and HhaI were simultaneously used in cluster analysis. The resultant dendrogram

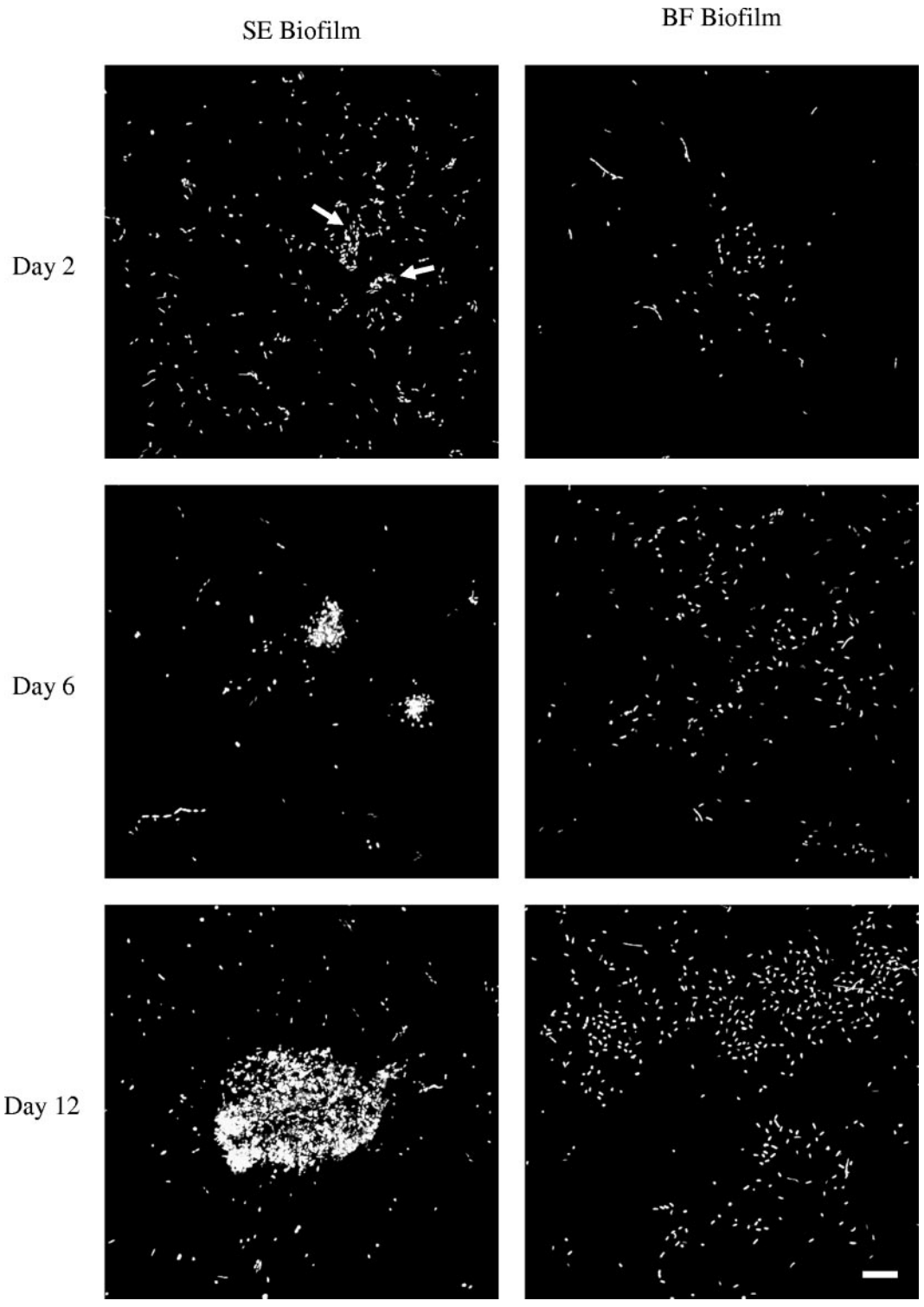

FIG. 3. Development of biofilms cultivated from secondary effluent and biofilter effluent on glass substrata. The bar represents 10 μm for all microscopic images. The white arrows indicate microcolonies.

(Fig. 8) showed that BF_6 to BF_12 formed a single cluster separate from the rest of the samples. SE_2, BF_2, and BF_4 were also grouped together, away from the distinct SE biofilm cluster.

In order to assign phylogenetic identities to the dominant peaks encountered in the community T-RFLP fingerprints, phylotypes from *Proteobacteria* and the CFB cluster were digested with MspI, RsaI, and HhaI to obtain their correspond-

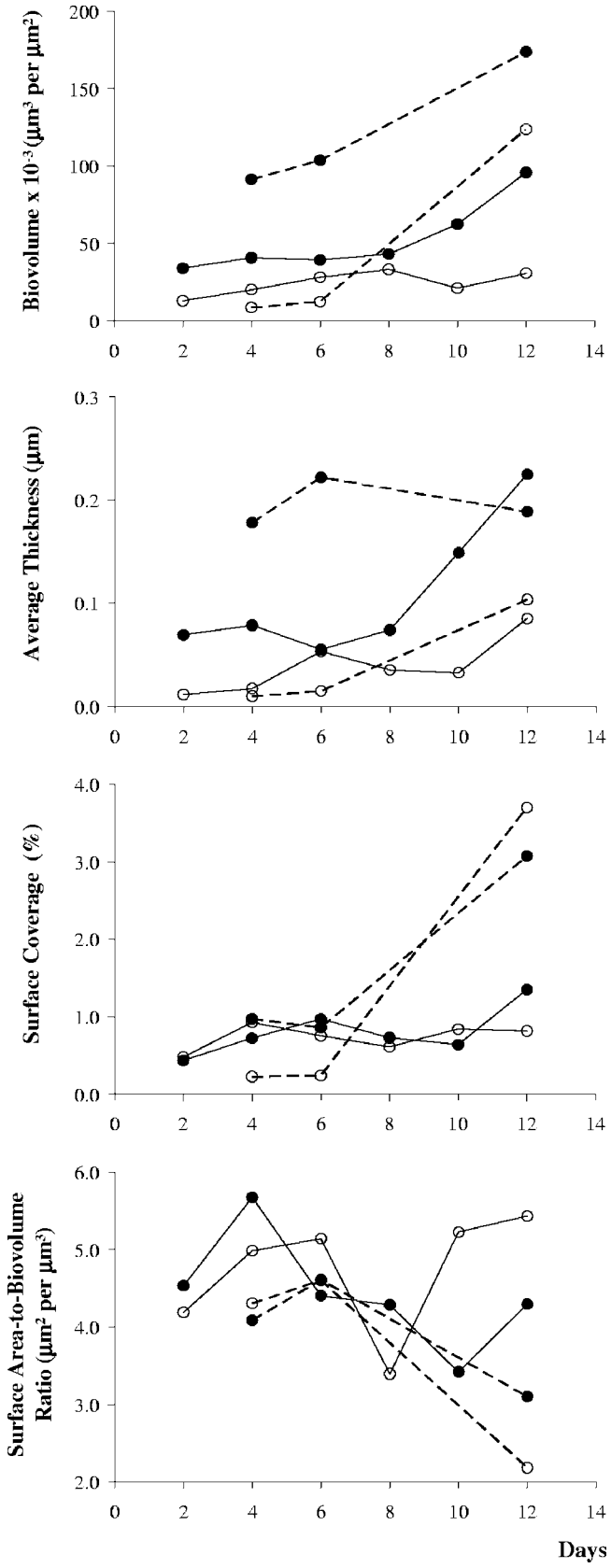

FIG. 4. Quantitative biofilm parameters for biofilms developed in run 1 (– – –) and run 2 (—) using secondary effluent (●) and biofilter effluent (○).

ing T-RFs (Fig. 6). Based on MspI digestion analyses (Fig. 7), the dominant 111-bp T-RF represented alphaproteobacterial phylotypes related to the *Sphingomonadaceae* (SE11, SE48, SE94, and BF84) and the *Caulobacteraceae* (SE63 and BF22). These phylotypes also contributed to the dominant 382-bp T-RF in community fingerprints produced by RsaI. Another major peak encountered in both biofilm samples was the 448-bp T-RF, which corresponded to *Acidovorax* (SE191 and BF192) in *Betaproteobacteria*. Other betaproteobacterial phylotypes in the SE_10 biofilm produced T-RFs of 401 and 451 bp, while those from the BF_10 biofilm were associated with T-RFs of 100, 451, 453, and 455 bp. A 453-bp T-RF was also detected in the SE_10 biofilm but was found to correspond to a gammaproteobacterium instead. This contrasted with those in the BF_10 biofilm, which were associated with T-RFs of 130 and 459 bp.

DISCUSSION

The reduction of bacterial growth and biological fouling by organic-carbon and nutrient removal has enjoyed widespread acceptance in industrial and process engineering. Earlier studies investigating the impact of organic carbon perturbations on biofilm development often associated a reduction in the availability of a growth-related substrate to biofilms that were thinner and contained less biomass than those growing under nutritionally sufficient conditions (16, 36). Likewise, our data obtained from microtiter plate experiments showed that the A_{600}s in carbon-impoverished BF biofilms were significantly lower than those in SE biofilms. Because of this well-established relationship, the quantification of the organic-carbon content and its various important constituents, like AOC, has been used extensively in biofilm monitoring. However, the general usefulness of AOC is limited by the complexity and low speed involved in its determination. Furthermore, the use of pure-culture inocula of *Pseudomonas fluorescens* P17 and *Spirillum* sp. strain NOX is innately controversial, and an alternative using a natural microbial consortium has been suggested (14).

The microtiter plate assay described here avoids the drawbacks associated with these bioassays. The biofilm formation potential of a water sample can be assessed directly in less than 2 h by using indigenous microorganisms, which form biofilms on the walls and at the bottom of each well. A high R^2 value between the A_{600} and biovolume measurements further suggests that this assay provides representative biomass estimates, because the biovolume was independently determined using intact biofilm samples collected by polyacrylamide gel embedding (10).

In the process of biofilm development, surface colonization is known to proceed by motility-assisted locomotion (15) or clonal growth (42). In the latter case, distinct patterns of colonization behavior, including spreading, shedding, and packing maneuvers, have been described (23). Microcolonies produced by spreading tend to be poorly defined, with cell-to-cell separation reaching as much as 5 to 20 μm. Shedding does not produce microcolonies, because daughter cells move away from the immediate vicinity to colonize a new location. Surface colonization by these two maneuvers thus produces an unstructured assortment of single cells distributed over the surface—a pattern resembling the random arrangement of individual cells

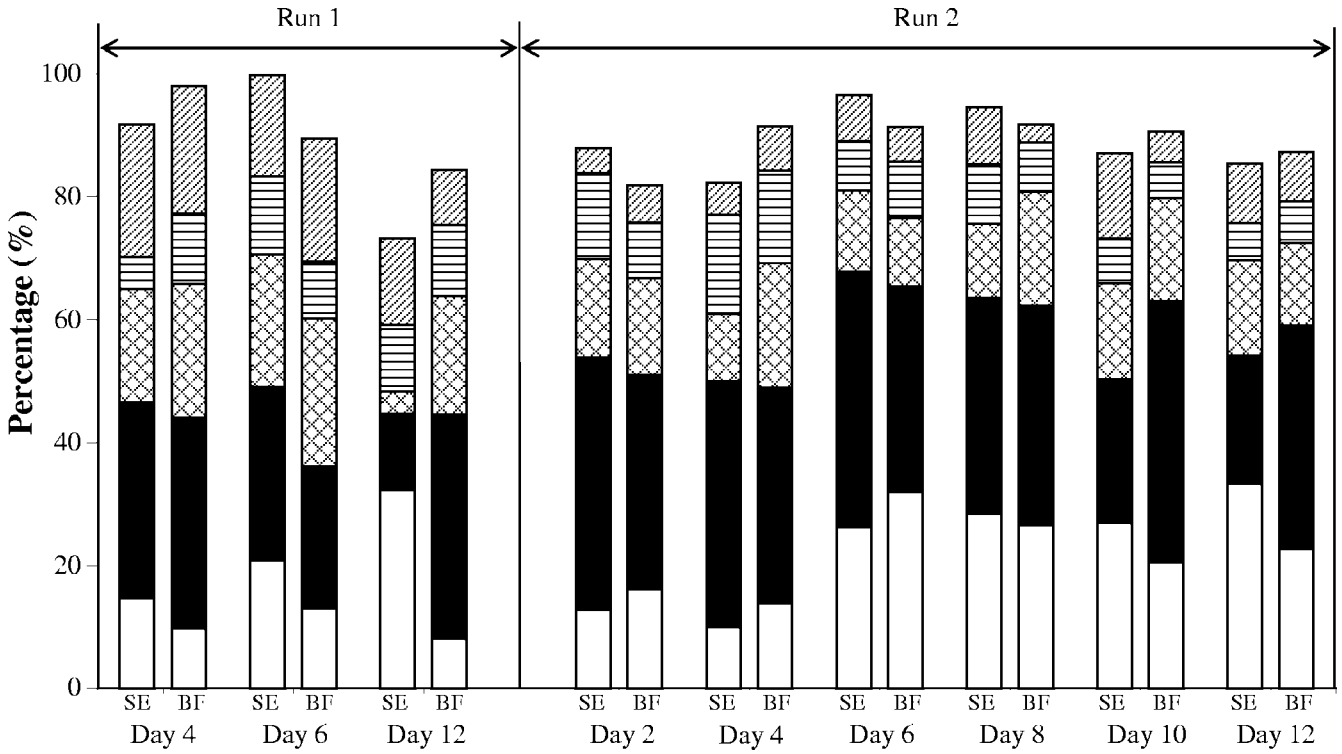

FIG. 5. Biofilm community compositions as revealed by FISH for biofilms developed in runs 1 and 2 on SE and BF. The biovolume obtained for each taxonomic group was expressed as a percentage of the total biovolume obtained by SYTO 9 staining. □, *Alphaproteobacteria*; ■, *Betaproteobacteria*; ▩, *Gammaproteobacteria*; ▤, *Cytophaga-Flexibacter-Bacteroides* cluster; ▨, *Actinobacteria*.

in the monolayers of BF biofilms. In contrast, microcolonies produced by packing tend to be dendritic and compact. This characteristic was observed in the SE_2 biofilm, where compact microcolonies (Fig. 3) were produced by some SE members, as well as in laboratory-cultured *P. fluorescens* biofilms (24) and naturally occurring pond water biofilms (7). However, the appearance of different morphotypes when microcolonies developed into larger aggregates suggests that recruitment of secondary microorganisms is also significant in the development of SE biofilms.

Biofilm structural development and the resultant architecture have often been associated with substrate availability. Mathematical models (37, 44) relate a decrease in nutrient availability to an increase in biofilm porosity, and this was repeatedly shown in mixed-community biofilms (34, 43). Likewise, the BF_12 biofilm in run 2, consisting of a cell monolayer with low surface coverage and a high *S*/*B* ratio (Fig. 4), suggests that an open architecture with a probable optimized cell-to-cell separation was maintained in the BF biofilm. This adaptation maximizes the cells' surface area exposed to the nutrient flow and reduces resource competition in a carbon-restricted environment. However, the relationship between substrate availability and biofilm architecture is not always predictable. In run 1, the porosity of BF_12 biofilms appeared to be lower than that of the corresponding SE_12 biofilms. This discrepancy has also been noted in *P. aureofaciens* and *Acinetobacter* biofilms (16, 17) cultivated under different carbon concentrations. The apparent inconsistency in these results suggests that the biofilm architecture may have been influenced by microenvironmental conditions, such as the localized concentration gradient of substrates in the hydrodynamic boundary layer. Further research using microelectrode probes to examine localized microenvironments (34) is anticipated to provide valuable data for the elucidation of this relationship.

In addition to the effect on biofilm development, environmental perturbations in the availability of organic-carbon sources can also lead to the selection of distinct biofilm communities (22). Using T-RFLP, a temporal change in the community structure or bacterial succession was observed in both SE and BF biofilm communities. This phenomenon has been well researched in human dental biofilms, where biofilm formation is initiated predominantly by a defined group of pioneer colonizers consisting of actinomycetes and streptococci (28). Similarly, the emergence of pioneer colonizers was observed here, and they appeared to be common to both SE- and BF-cultivated biofilms. Selection for pioneer colonizers is probably not affected by the organic-carbon content but by the ability to adhere to the substratum, which can be dependent on several physicochemical parameters (6). The ability to produce exopolysaccharides can also enhance cellular adhesion, and this physiological trait is common among many members of the *Sphingomonadaceae* (5). Other cellular appendages, such as the prostheca on *Caulobacter* cells, are also known to mediate bacterial attachment. Together with the putative identification of the 111-bp T-RF in the SE_2 and BF_2 biofilms, *Sphingomonadaceae*- and *Caulobacter*-related organisms thus appear to be potential primary colonizers in these biofilms.

Following initial colonization, a subsequent loss of species

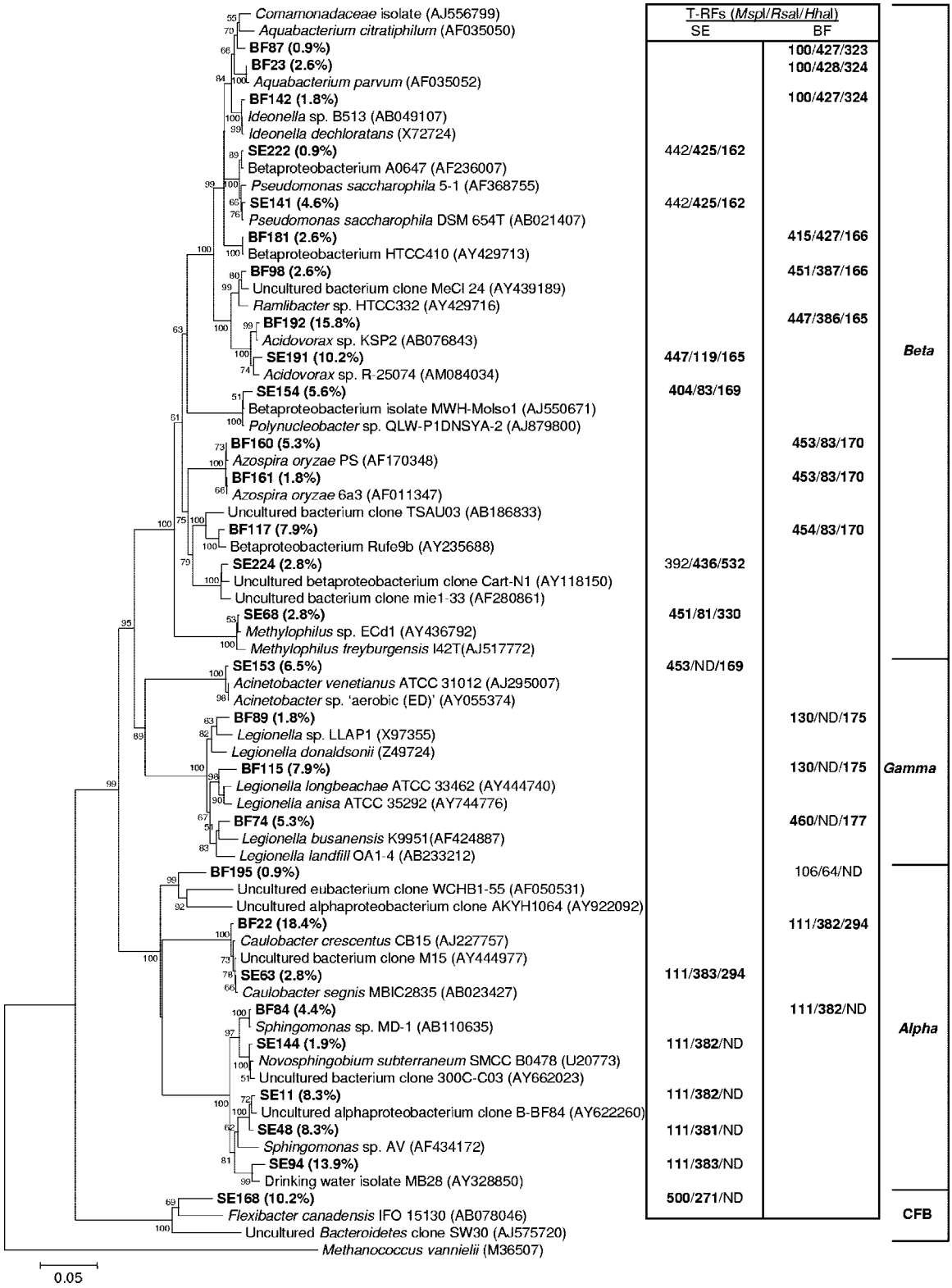

FIG. 6. Phylogenetic affiliations of 16S rRNA gene sequences retrieved from cloning analyses of SE_10 and BF_10 biofilms. The phylogenetic tree was constructed using a neighbor-joining algorithm with the Jukes-Cantor distance in MEGA3. The 16S rRNA gene sequence of *Methanococcus vannielii* (M36507) was selected as the outgroup. Bootstrap (n = 1,000) values of greater than 50% of the replicates are shown at the nodes. The abundances of individual clones are shown in parentheses. The bar indicates 1 substitution per 20 nucleotides. T-RFs of phylotypes digested with MspI, RsaI, and HhaI are also shown, and those in boldface could be assigned to a peak in the community T-RFLP fingerprints.

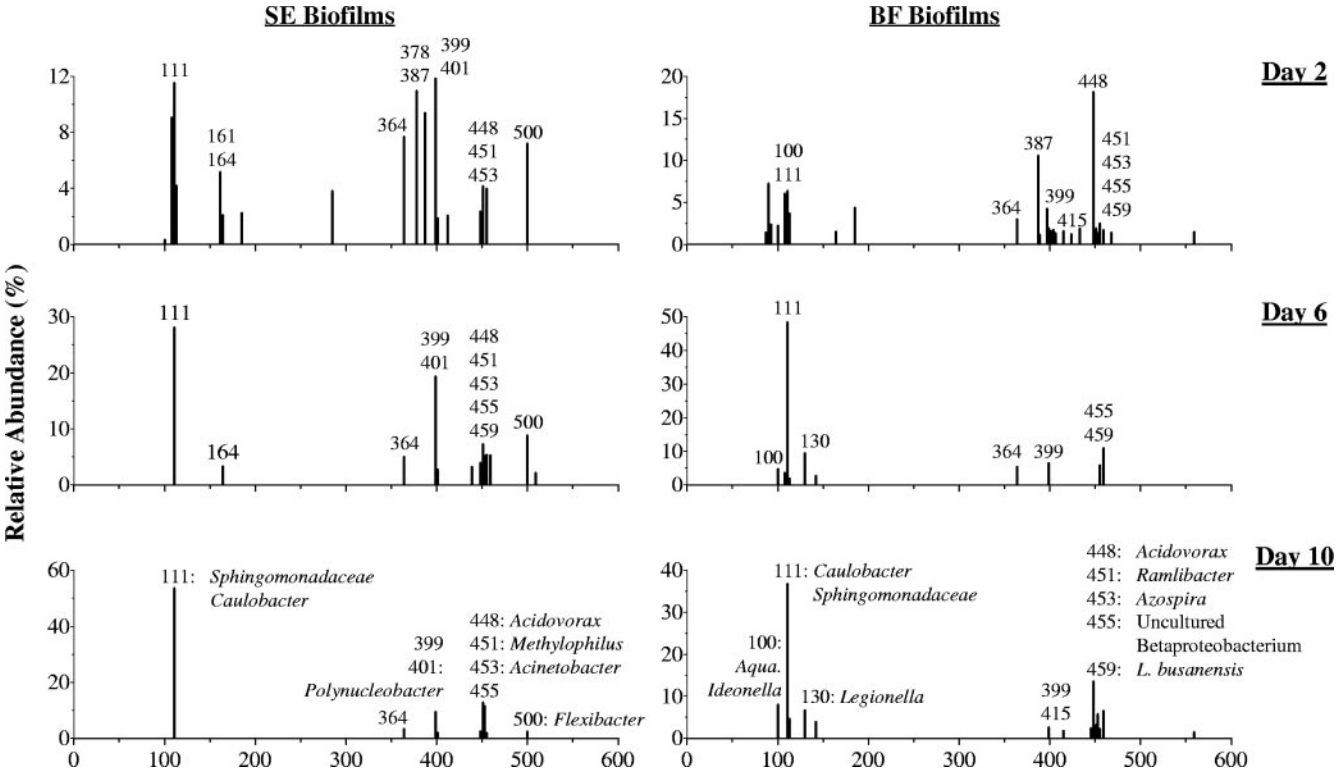

FIG. 7. T-RFLP profiles obtained from the biofilm samples collected in run 2 on days 2, 6, and 10 and digested with the restriction enzyme MspI. The relative abundance of each fragment was computed by expressing the associated peak area as a percentage of the total peak area for all fragments. *Aqua*., *Aquabacterium*.

richness suggests that competitive interactions exist between biofilm organisms in which some pioneer colonizers are outcompeted. As the ecological conditions in the SE and BF habitats were not the same, organisms with different physiological characteristics were selected in the two biofilms. For example, the 100-bp T-RF in the BF biofilms was associated with phylotypes related to *Aquabacterium*. This genus is typically found in oligotrophic environments, like drinking water systems (18), where bacterial activity can be severely restricted by low contents of organic carbon (25) and, possibly, phosphorus (32). The proliferation of *Aquabacterium* phylotypes in BF biofilms suggests that biofiltration exerts a selection pressure that favors the growth of organisms physiologically adapted for survival under low-nutrient conditions. This was further supported by the exclusive occurrence of phylotypes BF74, BF89, and BF115, closely related to *Legionella*, a genus that is often found in oligotrophic freshwater and drinking water biofilms (4).

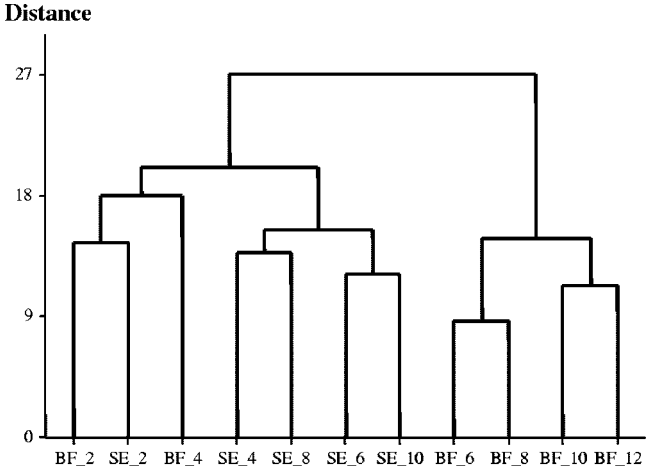

FIG. 8. Cluster analysis of T-RFLP fingerprints of SE and BF biofilms. The Euclidean distance was computed after square root transformation of the relative abundance for each T-RF and was joined by Ward's method.

To adapt to low-nutrient conditions, some organisms selected for in the BF habitat also appeared to be metabolically versatile. Phylotypes (BF160 and BF161) associated with the 453-bp T-RF were related to *Azospira oryzae*, which is known to fix nitrogen (39). These phylotypes were present only in the BF biofilms, suggesting that nitrogen fixation can be an important mode of cellular growth in localized microenvironments where microaerobic conditions prevailed in the biofilm. The ability to fix dinitrogen as a source of cell nitrogen freed these phylotypes from dependence on fixed forms of nitrogen (like ammonia) and thus conferred an ecological advantage for their survival in a nutrient-limited environment.

Despite the different ecological pressures in the SE and BF niches, certain groups of bacteria continued to thrive in both biofilm communities. This was exemplified by the increase in abundance of the 111-bp T-RF, possibly representing either the *Sphingomonadaceae* or *Caulobacter* spp. in *Alphaproteobac-*

teria. Alphaproteobacterial populations were also selectively enriched at a higher rate in SE- than in BF-cultivated biofilms. This suggests that although the growth of these alphaproteobacterial populations was affected by the removal of organic carbon by biofiltration, they could still compete favorably with other biofilm bacteria, presumably due to their ability to catabolize a large variety of organic substrates (5, 38). For example, *Caulobacter* spp., which are known to survive under low-nutrient conditions (38), were found to be dominant in the BF_10 biofilm but not in the SE_10 biofilm.

Although the effect of the organic-carbon concentration on biofilm formation has been well established, this study suggests that the correlation may not be a simple one, due to the selection of biofilm organisms that are adapted for survival under low-substrate conditions. These organisms, including those with low nutritional requirements (e.g., *Aquabacterium*, *Caulobacter*, and *Legionella*) and others that are metabolically versatile (*Azospira* and sphingomonads), tend to form open biofilm structures that maximize the influx of nutrients into the biofilm. These adaptive strategies imply that carbon limitation may not be an effective barrier to biofilm growth. For this reason, long-term biofouling control may not be achievable using carbon limitation strategies alone, and it would thus be prudent to assess the biofilm formation potential of a water sample by using a combination of organic-carbon-based measurements and direct biofilm quantification. As described above, the microtiter plate assay is a powerful tool for direct biomass determination in terms of speed, simplicity, and representation. In the same way, the molecular analyses of temporal biofilm communities can uncover useful information for the formulation of specific countermeasures. For example, biofouling caused by SE effluents may be more appropriately dispersed by a mixture of polysaccharidases than by conventional oxidizing biocides, as *Sphingomonadaceae*-related organisms are likely to form exopolysaccharide-ensconced biofilms. When incorporated as a side stream device, the techniques described here are expected to provide insight into biofilms developed on inaccessible locations (such as on the interior surfaces of reverse-osmosis membranes) and to assist in the timely mitigation of biofouling.

ACKNOWLEDGMENTS

We thank Huiling Guo, Sim Yi Koh, Chia-Lung Chen, and Fea Mein Tan for experimental support.

Chee Meng Pang is supported by a scholarship from the Singapore Millennium Foundation.

REFERENCES

1. **Altschul, S. F., T. L. Madden, A. A. Schaffer, J. Zhang, Z. Zhang, W. Miller, and D. J. Lipman.** 1997. Gapped BLAST and PSI-BLAST: a new generation of protein database search programs. Nucleic Acids Res. **25:**3389–3402.
2. **American Public Health Association, American Water Works Association, and Water Environment Federation.** 1998. Standard methods for the examination of water and wastewater, 20th ed. United Book Press Inc., Washington, D.C.
3. **Ashelford, K. E., N. A. Chuzhanova, J. C. Fry, A. J. Jones, and A. J. Weightman.** 2005. At least 1 in 20 16S rRNA sequence records currently held in public repositories is estimated to contain substantial anomalies. Appl. Environ. Microbiol. **71:**7724–7736.
4. **Atlas, R. M.** 1999. *Legionella*: from environmental habitats to disease pathology, detection and control. Environ. Microbiol. **1:**283–293.
5. **Balkwill, D. L., J. K. Fredrickson, and M. F. Rominem.** 31 July 2003, posting date. *Sphingomonas* and related genera. *In* M. Dworkin et al. (ed.), The prokaryotes: an evolving electronic resource for the microbiological community. Springer-Verlag, New York, N.Y. [Online.] http://141.150.157.117:8080/prokPUB/chaprender/jsp/showchap.jsp?chapnum=314&initsec=02_00.
6. **Bos, R., H. C. van der Mei, and H. J. Busscher.** 1999. Physico-chemistry of initial microbial adhesive interactions—its mechanisms and methods for study. FEMS Microbiol. Rev. **23:**179–230.
7. **Bott, T. L., and T. D. Brock.** 1970. Growth and metabolism of periphytic bacteria: methodology. Limnol. Oceanogr. **15:**333–342.
8. **Camper, A. K.** 2000. Biofilms in drinking water treatment and distribution, p. 311–332. *In* L. V. Evans (ed.), Biofilms: recent advances in their study and control. Harwood Academic Publishers, Amsterdam, The Netherlands.
9. **Chen, C. L., H. Macarie, I. Ramirez, A. Olmos, S. L. Ong, O. Monroy, and W. T. Liu.** 2004. Microbial community structure in a thermophilic anaerobic hybrid reactor degrading terephthalate. Microbiology **150:**3429–3440.
10. **Christensen, B. B., C. Sternberg, J. B. Andersen, R. J. Palmer, Jr., A. T. Nielsen, M. Givskov, and S. Molin.** 1999. Molecular tools for study of biofilm physiology. Methods Enzymol. **310:**20–42.
11. **Costerton, J. W., Z. Lewandowski, D. E. Caldwell, D. R. Korber, and H. M. Lappin-Scott.** 1995. Microbial biofilms. Annu. Rev. Microbiol. **49:**711–745.
12. **Djordjevic, D., M. Wiedmann, and L. A. McLandsborough.** 2002. Microtiter plate assay for assessment of *Listeria monocytogenes* biofilm formation. Appl. Environ. Microbiol. **68:**2950–2958.
13. **Egert, M., and M. W. Friedrich.** 2003. Formation of pseudo-terminal restriction fragments, a PCR-related bias affecting terminal restriction fragment length polymorphism analysis of microbial community structure. Appl. Environ. Microbiol. **69:**2555–2562.
14. **Hammes, F. A., and T. Egli.** 2005. New method for assimilable organic carbon determination using flow-cytometric enumeration and a natural microbial consortium as inoculum. Environ. Sci. Technol. **39:**3289–3294.
15. **Harshey, R. M.** 2003. Bacterial motility on a surface: many ways to a common goal. Annu. Rev. Microbiol. **57:**249–273.
16. **Heydorn, A., A. T. Nielsen, M. Hentzer, C. Sternberg, M. Givskov, B. K. Ersboll, and S. Molin.** 2000. Quantification of biofilm structures by the novel computer program COMSTAT. Microbiology **146:**2395–2407.
17. **James, G. A., D. R. Korber, D. E. Caldwell, and J. W. Costerton.** 1995. Digital image analysis of growth and starvation responses of a surface-colonizing *Acinetobacter* sp. J. Bacteriol. **177:**907–915.
18. **Kalmbach, S., W. Manz, J. Wecke, and U. Szewzyk.** 1999. *Aquabacterium* gen. nov., with description of *Aquabacterium citratiphilum* sp. nov., *Aquabacterium parvum* sp. nov. and *Aquabacterium commune* sp. nov., three in situ dominant bacterial species from the Berlin drinking water system. Int. J. Syst. Bacteriol. **49:**769–777.
19. **Karthikeyan, S., D. R. Korber, G. M. Wolfaardt, and D. E. Caldwell.** 2001. Adaptation of bacterial communities to environmental transitions from labile to refractory substrates. Int. Microbiol. **4:**73–80.
20. **Korber, D. R., J. R. Lawrence, M. J. Hendry, and D. E. Caldwell.** 1992. Programs for determining statistically representative areas of microbial biofilms. Binary **4:**204–210.
21. **Kumar, S., K. Tamura, and M. Nei.** 2004. MEGA3: integrated software for molecular evolutionary genetics analysis and sequence alignment. Brief Bioinform. **5:**150–163.
22. **LaPara, T. M., T. Zakharova, C. H. Nakatsu, and A. Konopka.** 2002. Functional and structural adaptations of bacterial communities growing on particulate substrates under stringent nutrient limitation. Microb. Ecol. **44:**317–326.
23. **Lawrence, J. R., and D. E. Caldwell.** 1987. Behavior of bacterial stream populations within the hydrodynamic boundary layers of surface microenvironments. Microb. Ecol. **14:**15–28.
24. **Lawrence, J. R., P. J. Delaquis, D. R. Korber, and D. E. Caldwell.** 1987. Behavior of *Pseudomonas fluorescens* within the hydrodynamic boundary layers of surface microenvironments. Microb. Ecol. **14:**1–14.
25. **LeChevallier, M. W., T. M. Babcock, and R. G. Lee.** 1987. Examination and characterization of distribution system biofilms. Appl. Environ. Microbiol. **53:**2714–2724.
26. **Lechevallier, M. W., N. E. Shaw, L. A. Kaplan, and T. L. Bott.** 1993. Development of a rapid assimilable organic-carbon method for water. Appl. Environ. Microbiol. **59:**1526–1531.
27. **Legendre, P., and E. D. Gallagher.** 2001. Ecologically meaningful transformations for ordination of species data. Oecologia **129:**271–280.
28. **Li, J., E. J. Helmerhorst, C. W. Leone, R. F. Troxler, T. Yaskell, A. D. Haffajee, S. S. Socransky, and F. G. Oppenheim.** 2004. Identification of early microbial colonizers in human dental biofilm. J. Appl. Microbiol. **97:**1311–1318.
29. **Liu, W.-T., C. L. Huang, J. Y. Hu, L. F. Song, S. L. Ong, and W. J. Ng.** 2002. Denaturing gradient gel electrophoresis polymorphism for rapid 16S rDNA clone screening and microbial diversity study. J. Biosci. Bioeng. **93:**101–103.
30. **Liu, W.-T., T. L. Marsh, H. Cheng, and L. J. Forney.** 1997. Characterization of microbial diversity by determining terminal restriction fragment length polymorphisms of genes encoding 16S rRNA. Appl. Environ. Microbiol. **63:**4516–4522.
31. **Maidak, B. L., J. R. Cole, T. G. Lilburn, C. T. Parker, Jr., P. R. Saxman, J. M. Stredwick, G. M. Garrity, B. Li, G. J. Olsen, S. Pramanik, T. M. Schmidt, and J. M. Tiedje.** 2000. The RDP (Ribosomal Database Project) continues. Nucleic Acids Res. **28:**173–174.

32. **Miettinen, I. T., T. Vartiainen, and P. J. Martikainen.** 1997. Phosphorus and bacterial growth in drinking water. Appl. Environ. Microbiol. **63:**3242–3245.
33. **Norton, C. D., and M. W. LeChevallier.** 2000. A pilot study of bacteriological population changes through potable water treatment and distribution. Appl. Environ. Microbiol. **66:**268–276.
34. **Okabe, S., T. Kindaichi, T. Ito, and H. Satoh.** 2004. Analysis of size distribution and areal cell density of ammonia-oxidizing bacterial microcolonies in relation to substrate microprofiles in biofilms. Biotechnol. Bioeng. **85:**86–95.
35. **O'Toole, G. A., and R. Kolter.** 1998. Initiation of biofilm formation in *Pseudomonas fluorescens* WCS365 proceeds via multiple, convergent signalling pathways: a genetic analysis. Mol. Microbiol. **28:**449–461.
36. **Peyton, B. M.** 1996. Effects of shear stress and substrate loading rate on *Pseudomonas aeruginosa* biofilm thickness and density. Water Res. **30:**29–36.
37. **Picioreanu, C., M. C. M. van Loosdrecht, and J. J. Heijnen.** 1998. Mathematical modeling of biofilm structure with a hybrid differential-discrete cellular automaton approach. Biotechnol. Bioeng. **58:**101–116.
38. **Poindexter, J. S.** 21 May 1999, posting date. Dimorphic prosthecate bacteria: the genera *Caulobacter*, *Asticcacaulis*, *Hyphomicrobium*, *Pedomicrobium*, *Hyphomonas*, and *Thiodendron*. *In* M. Dworkin et al. (ed.), The prokaryotes: an evolving electronic resource for the microbiological community. Springer-Verlag, New York, N.Y. [Online.] http://141.150.157.117:8080/prokPUB/chaprender/jsp/showchap.jsp?chapnum=106&initsec=02_00.
39. **Reinhold-Hurek, B., and T. Hurek.** 2000. Reassessment of the taxonomic structure of the diazotrophic genus *Azoarcus* sensu lato and description of three new genera and new species, *Azovibrio restrictus* gen. nov., sp. nov., *Azospira oryzae* gen. nov., sp. nov. and *Azonexus fungiphilus* gen. nov., sp. nov. Int. J. Syst. Evol. Microbiol. **50:**649–659.
40. **Ridgway, H. F., and H.-C. Flemming.** 1996. Membrane biofouling, p. 6.1–6.62. *In* J. Mallevialle, P. E. Odendaal, and M. R. Wiesner (ed.), Water treatment membrane processes. McGraw-Hill, New York, N.Y.
41. **Stoodley, P., I. Dodds, J. D. Boyle, and H. M. Lappin-Scott.** 1998. Influence of hydrodynamics and nutrients on biofilm structure. J. Appl. Microbiol. **85:**19S–28S.
42. **Tolker-Nielsen, T., U. C. Brinch, P. C. Ragas, J. B. Andersen, C. S. Jacobsen, and S. Molin.** 2000. Development and dynamics of *Pseudomonas* sp. biofilms. J. Bacteriol. **182:**6482–6489.
43. **Wijeyekoon, S., T. Mino, H. Satoh, and T. Matsuo.** 2004. Effects of substrate loading rate on biofilm structure. Water Res. **38:**2479–2488.
44. **Wimpenny, J. W. T., and R. Colasanti.** 1997. A unifying hypothesis for the structure of microbial biofilms based on cellular automaton models. FEMS Microbiol. Ecol. **22:**1–16.
45. **Wong, M. T., F. M. Tan, W. J. Ng, and W.-T. Liu.** 2004. Identification and occurrence of tetrad-forming *Alphaproteobacteria* in anaerobic-aerobic activated sludge processes. Microbiology **150:**3741–3748.